Journal of
Composites Science

MDPI

Article

Piezoresistive and Mechanical Behavior of CNT Based Polyurethane Foam

Enea De Meo [1,2], Simone Agnelli [1], Antonino Veca [2], Valentia Brunella [1] and Marco Zanetti [1,3,*]

1 Department of Chemistry, NIS and INSTM Reference Centres, University of Torino, Via P. Giuria 7, 10125 Torino, Italy; enea.demeo@unito.it (E.D.M.); simone.agnelli@edu.unito.it (S.A.); valentina.brunella@unito.it (V.B.)
2 Centro Ricerche Fiat. S.C.p.A.—Group Materials Labs, C.so Settembrini 40, 10135 Torino, Italy; antonino.veca@crf.it
3 ICxT Centre, University of Torino, Lungo Dora Siena 100, 10153 Torino, Italy
* Correspondence: marco.zanetti@unito.it

Received: 31 July 2020; Accepted: 2 September 2020; Published: 6 September 2020

Abstract: Carbon nanotubes (CNT) embedded into a polymeric foam demonstrate an enhancement in electrical and mechanical properties of the final nanocomposite. The enhanced material with new characteristics, e.g., piezoresistivity, can be substituted with the traditional metallic material to design sensors, switches, and knobs directly into a single multifunctional component. Research activities in this field are moving towards a mono-material fully integrated smarts components. In order to achieve this goal, a simple method is developed to produce piezoresistive polyurethane/CNT foams. The novelty consists in applying the dispersion of CNT considering industrial production constrains, in order to facilitate its introduction into a common industrial practice. Three kinds of PU-CNT foam have been prepared and tested: PU-CNT 1.5%, PU-CNT-COOH 1.0%, and PU-CNT-COOH 1.5%. Polyurethane with CNT-COOH showed an insulating-conductive transition phenomenon when the foam reaches the 80% of its compression strain with a Gauge factor (Gf) of about 30. Instead, PU-CNT showed conductivity only at 1.5% of filler concentration and a steady piezoresistive behavior with a Gf of 80. However, this samples did not show the insulating-conductive transition. Having improved the electromechanical properties of final nanocomposite polyurethane foam demonstrates that the proposed method can be applied differently for design sensors and switches.

Keywords: nanocomposite; conductive polymers; polymer-matrix composites (PMCs); electrical properties

1. Introduction

The automotive market is evolving towards smart vehicles where inter-vehicle communication systems support applications related to safety, comfort, info-mobility, and passenger entertainment. The current production of cars is subjected to implementation requests in terms of amount and typologies of human-machine interface (HMI), e.g., switches and adjustment knobs, placed mainly in the dashboard or door panels.

At present, most multi-material devices connected with metal wires represent the on-board vehicle electronic systems. Metal wires, buttons, and sensors are usually inserted in the plastic component, after moulding, and this increases manufacturing cost. Separation of metal and polymers for disposal or recycling is also an expensive procedure. Different strategies have been tried to obtain smart nanocomposite with different properties, like piezoresistivity (sensors) and conductivity (electrical connection). The most recent researches proved that adding carbon nanoparticles (such as graphene

nano platelets (GNP), or carbon black (CB), or carbon nanotubes (CNT)) to commercial polymer composites can provide an improvement of the mechanical behaviors [1–3], thermal conductivity [4,5], electric conductivity [6–9], and piezoresistive behavior [10–14].

The effect on the nanocomposite electric conductivity and piezoresistive behavior can be the results of the combination of high aspect ratios of CNT and the quantum channeling [15], which yields to the formation of continuous network structures in the polymer matrix [16,17]. The polymer composites containing CNT, or carbon nanoparticles, or both also showed piezoresistive behavior. Therefore, they were investigated for fabrication of stress, strain or pressure sensors [12–14,17–19].

Similar hybrid polymer composites with CNT and carbonaceous fillers showed shape memory performance [20]. Finally, it is well assessed that conductive CNT/polymer composites can be used to fabricate antennas, giving the possibility of setting up connections among the different parts in an easy and flexible way [21]. Conclusively, the achievement of the mentioned above functionalities greatly depends on the selected filler-matrix combination and on the composite manufacturing process. A significant number of matrixes and fillers have been tested to produce multifunctional nanocomposites. However, only a few numbers of polymers matrices already used in commercial automotive industry have been exploited as nanocomposite sensors. Polyurethane foams are extensively used in the construction of modern components: dashboard, steering wheel and door panel. Semi-rigid polyurethane has shown unique advantages including: lightweight, good manufacturability, inexpensive, high formability, and outstanding resilience performance. Polymer synthesis with conductive carbonaceous filler allows a tuning of the nanocomposite features. For instance, scientists have obtained a rigid polyurethane foam with electrical percolation at CNT loading of 2%wt. [22]. They discovered that the percolation at fixed concentration depends on the density of the polyurethane. In the case of a density of 0.05 g cm^{-3}, the CNT populates the cell strut, and the final foam becomes conductive.

The percolation of the polyurethane foam strongly depends on the morphological and structural property of the cell the cell-strut network. The polyurethane/CNT showed also a remarkable thermal stabilization of the matrix already at concentration of 0.5 wt% [23]. Scientists developed polyurethane/CNT composites with different weight percentage from 0.5 wt% to 2 wt% of CNT. The thermogravimetric analysis of neat polyurethane (PU) and PU/CNT showed differences. The onset of thermal decomposition for the nanocomposites shifted to a higher temperature respect to the neat polyurethane. In particular, the degradation temperature increased by 50 °C for 50 % weight loss for PU/CNT 0.5%, with respect to neat PU [23]. In literature, it is reported that piezoresistive behavior of semi-rigid expanded polyurethane/CNT with open cells is obtained mainly by dipping the cured foam in a solution made of solvent and well dispersed CNT, and then the wet foam is dried into an oven for solvent evaporation. The final sample is a foam in which the external part of the cells is filled with CNT. For instance, Amit Tewari et al. [24] produced a piezoresistive polyurethane sponge by dipping a commercial PU sponge into a reduced graphene oxide/CNT ink. The final sensor has subjected to 5000 cycles without losing electrical properties. However, this kind of procedure is not suitable in a large-scale production. Furthermore, in-situ preparation seems to be more suitable for market demand. For instance, scientists obtained a piezoresistive polyurethane foam by mixing the polyol solution with CNT and final adding the PM-200 diisocyanate. Moreover, the scientists characterized the piezoresistive performance of the resulting nanocomposite foam with compressive mechanical test while the electric resistance was acquired [25].

The sample with 1 wt % of CNT showed piezoresistive properties only when the sample was compressed between the 0% and 40% of the compressive strain. In this research, the highest gauge factor was obtained only when the conductive network inside the material was not completely formed, which means when the CNT weight percentage was lower than the percolation. Scientists showed that the conductive fillers approach each other causing an increase of the conductivity with the compression and pull away with the relaxation causing a decrease of the conductivity. The "resistance relaxation" phenomenon induces a progressive signal drift of the electrical resistance while the foam is subjected

to cyclic tests. The objective of this research is to develop a simple method to produce piezoresistive polyurethane foam starting from a two-component commercial preparation extensively used in the main production chain of different goods. The final nanocomposite foam should show a stable piezoresistive effect under cyclic deformation in order to replace multi-materials electronic switches, handles, and knobs inside plastics components (automotive dashboard, household appliance, home automation). The novelty under this approach is to make multi-components goods, like cars, washing machines, etc., more recyclable and simpler or, rather, lowering their environmental impact in terms of number of non-renewable resources used. To achieve this goal, we developed a specific polyurethane/CNT formulation to obtain a foam with mechanical characteristics similar to commercial polyurethane foam, which is easy to produce and with a good processability. The final polyurethane foam is proposed as a pressure sensor, simultaneously maintaining the aesthetic purpose and giving a softness tactile feeling. PU is well known as an insulating material, and a conductive filler is needed to obtain the piezoresistive effect. Multiwall CNT have been selected due to their excellent mechanical and electrical properties, their relatively low cost compared to other functional materials and single wall CNT, a higher aspect ratio than metal particles, and potential high affinity with polymer matrix. Moreover, functionalized CNT with COOH group have been used in order to evaluate the effect on mechanical and piezoresistive behavior respect to foam with non-functionalized CNT. We chose to use CNT-COOH, assuming the hypothesis that the functionalized nanotubes can disperse differently within the polyol and improve the piezoresistive and mechanical behavior of the final nanocomposite due to the fact that they could react with OH group. The polyurethane/CNT composite foams were also engineered to obtain pressure sensor and switches.

2. Materials and Methods

2.1. Formulation

PU foams were produced mixing a polyol formulation, including a catalyst, a foaming agent, a surfactant, and a polyol with di-isocyanate. The material used for preparing the PU foam was furnished and produced by BASF Italy, Villanova d'Asti (AT): Lupranol® 2007/1 as polyol, 1,4-Diazabicyclo[2.2.2]octane (DABCO) as a catalyst, Tegostab B 8715 LF2 as surfactant, distilled water as foaming agent, and Methylene diphenyl diisocyanate (MDI) as isocyanate.

In this work, Multiwall CNT were supplied by Nanostructured & Amorphous Materials, Inc. (NanoAmor, Katy, TX, USA). Two different kind of CNT were tested including: -COOH functionalized nanotubes and non-functionalized ones. Both fillers have a 50–80nm diameter, 10–20 μm length, and 95% wt. pureness.

2.2. Sample Preparation

Foam preparation begins with mixing CNT 0.16 g with 1 wt % or 0.24 g with 1.5 wt % with 10 g of the polyether polyol in a crusher. The solution was sonicated for 2 h, and then the obtained mixture was subjected to a mechanical stirring with a four–bladed rod for 1 hr with the rotational speed of 200 rpm to homogenize and brake CNT agglomerates by shear stress. During the second step, the surfactant (0.08 g), the foaming agent (0.59 g), and the catalyst (0.015 g) were added to the suspension. Finally, the obtained solution was poured into a cylindrical mould, and the isocyanate (5.6 g) was added and hand-mixed for 20 s. The final foam was then sliced with a blade into thinner disks of 4.5 cm diameter (D) and 1 cm thickness (thk) to obtain the final samples. In order to compare different samples, the specimens used for the electrical and mechanical characterizations were cut from the middle part of the foam, which was the area with highest homogeneity.

2.3. Mechanical Compression Tests

Compression tests were performed with a dynamometer Instron 5544 with a load cell of 2 kN. The Instron fixture for compression was composed with two metal cylinders of a diameter of 5 cm

(Figure 1). The method used for the mechanical characterization of the PU/CNT foam was a pure compression mode with displacement control and a deformation speed rate of 10 mm/min. All the samples were compressed from 0 to 99.98% of strain. Three samples for each foam was tested in order to have statistically relevant value. The elastic modulus in the plateau region was calculated by interpolating the compression curve with a straight line from 10% to 70% of strain, as in previous work [26]. All values were obtained by arithmetically averaging the values for each type of foam.

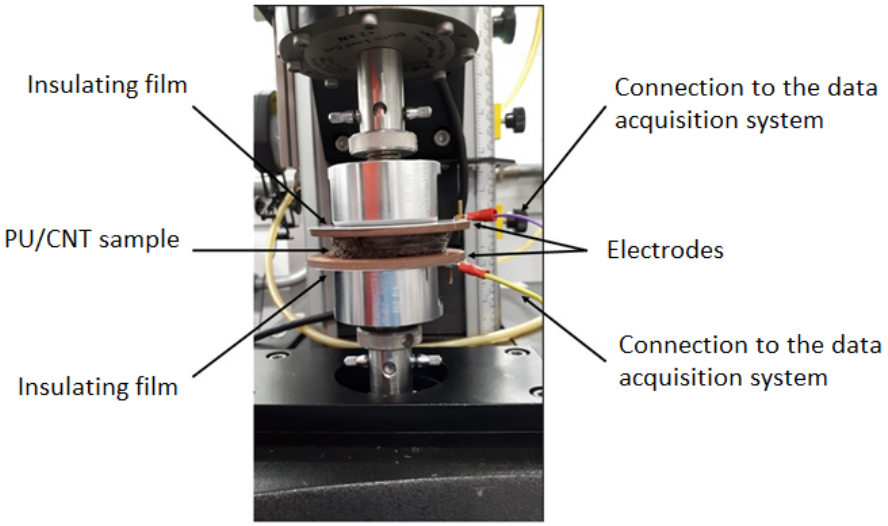

Figure 1. Digital image of the set-up used for piezoresistive characterization and mechanical compression.

2.4. Piezoresistive Characterizations

Piezoresistive characterization tests were conducted using a specific designed setup composed of a dynamometer Instron 5544 with a load cell of 2 kN, a potentiometer Gefran PY1 C 50 for direct acquisition of the strain, and a multi-meter Keithley KE2700 for the electrical resistance acquisition. Data acquisition board (cDAQ-9178, National Instruments, Austin, TX, USA) was connected to the multi-meter and the potentiometer for acquiring the information at the same instant. A LabVIEW software (National Instruments, Austin, TX, USA) was developed specifically for simultaneous data collection and elaboration. The samples were placed in between two copper electrodes (diameter: 5 cm and thickness of 0.5 cm); these metal plates were insulated with a thin plastic film made of Mylar® with the same diameter. The schematic of the experiment set-up for measuring piezoresistivity and compressive tests of the composite foam is shown in Figure 1. The electrodes were then connected to the multi-meter by electric wires. This setup can collect real time data of the electrical resistance versus applied deformation of the material.

2.5. Electronic Microscope

SEM images were taken to evaluate the presence of CNT inside foams, as mentioned before, and the samples were cryofractured and then sputtered with a thin gold layer with a 60-mA probe for 40 s, and the obtained film was 20–25 μm thick. The instrument used in this work was EVO XVP-LaB6 (Zeiss, Oberkochen, Germany) equipped with both secondary and backscattered electron sensors.

3. Results

3.1. SEM Images

In first place, SEM images of CNT were taken, as can be seen in Figure 2d, to observe the morphology of the particles. As the picture shows, it is possible to see single nanotubes, using secondary electrons

at 10k x magnification. CNT produced by NanoAmor have been well characterized and investigated in previous research works [26–29]. Later, the same analysis was performed on a neat sample (Figure 2a) to have a reference for further images. In every SEM image of CNT added samples, the presence of separated nanotubes can be observed. CNT are visible as tiny filaments emerging from the matrix surface. This is due to CNT higher mechanical properties respect to the matrix. CNT do not break when the foam is fractured, and their different morphology makes them visible using SEM microscopy. Figure 2b displays a SEM image of the PU/CNT 1.5 wt % (non-functionalized). The fillers were well dispersed inside the matrix, and any CNT agglomerates were found during the analysis. This indicates a high dispersion rate of CNT and a homogeneous morphology of the foam. Figure 2c shows an SEM image of PU/CNT-COOH 1.5%, and some CNT agglomerates, like the one shown in the picture, were found during the analysis. Generally, the agglomerates emerged from the fracture surface, indicating a lower rate of dispersion and a completely different interaction between the matrix and the filler. Thanks to SEM images, we could prove not only the effective presence of CNT in the matrix but also that it is possible to evaluate the differences in the dispersion rate cause by the functionalization of the filler. Nevertheless, we demonstrated that the dispersion rate was not the only factor influencing piezoresistive properties in an elastomeric PU foam.

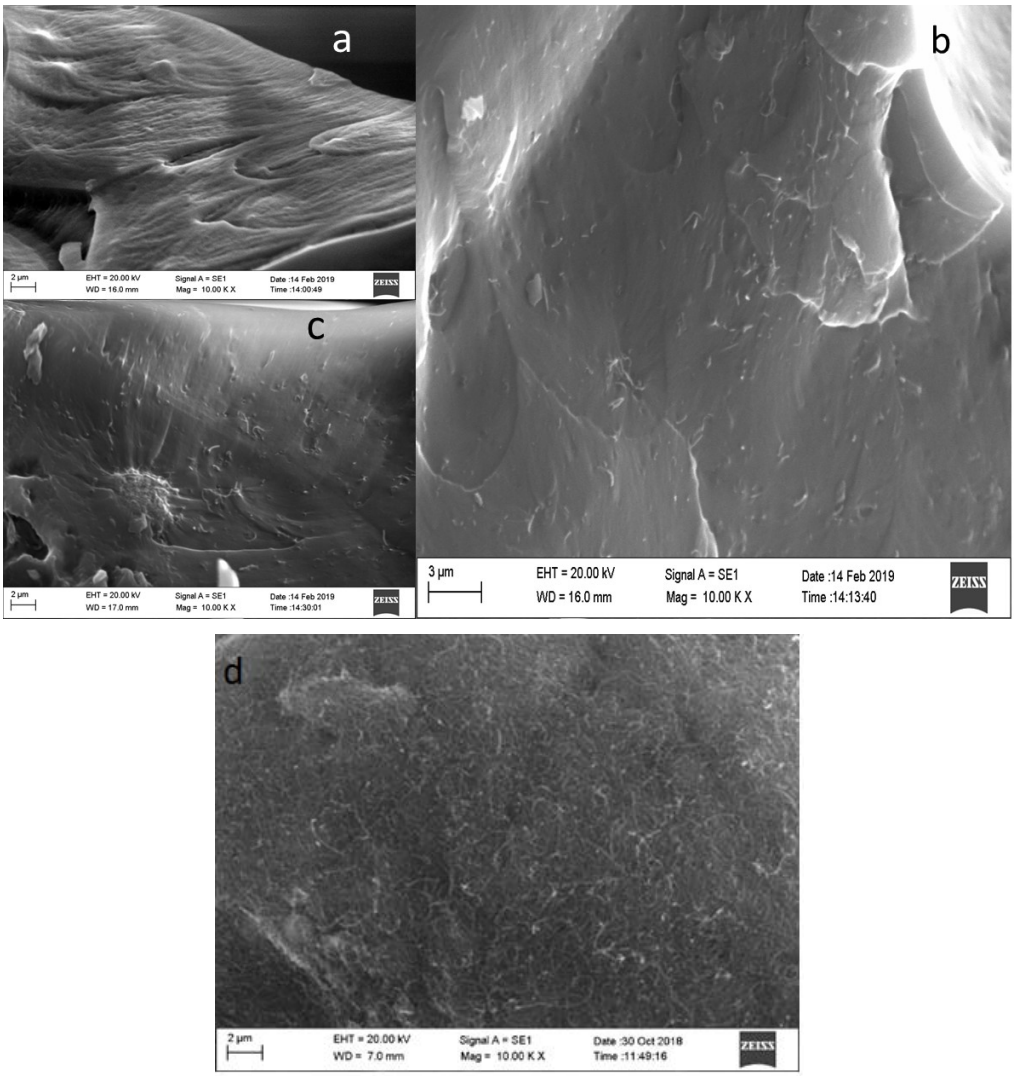

Figure 2. SEM images of polyurethane (PU) foam produced (**a**) neat PU, (**b**) PU/carbon nanotubes (CNT) 1.5%, (**c**) PU/CNT-COOH 1.5%, and (**d**) SEM image of CNT powder.

3.2. Compression Properties of the Composite Materials

Figure 3a shows the designed sandwich structure for the compressive tests in order to simulate the behavior of the foam under a finger pressure. The aim of this configuration design was to understand the role of the foam in the composite structure and the nature of the interaction with the PU foam. The polyurethane foam layer was placed between the polypropylene solid structure and the leather. The upper layer was a synthetic leather which has aesthetics purpose and to protect the substructure. To test the mechanical properties of solid polyurethane foams, compression tests are normally conducted. The sample was placed between compression platens (Instron fixture) connected to a dynamometer, and the applied pressure (σ) was measured as a function of the strain (ε). The result was a characteristic curve [30], shown in Figure 3b, which was obtained with a compression test of the neat polyurethane foam without being CNT produced, as described in previous section. According to the results obtained by Reference [30], it was possible to distinguish three different regions: I) Linear region: at low strain the foamed structure shows an elastic behavior and deforms linearly with the imposed compression, following the Hook's low; II) Stress plateau region: the microstructure of the foam reaches the Euler's critical load as the effect of a bifurcation of the equilibrium; and III) Exponential region: hardening effects, stress begins to rise exponentially with the deformation. One possible interpretation of this behavior considers a discontinuous model in which the cell structure has a bi-stable or two stables conformations one with low or zero stress levels and one with high stress levels. The linear behaviors correspond to the deformation of the first conformation; while a cell passes from the first structure to the second one, it absorbs an amount of energy that that is considered to be equal for all cells due to the homogeneous size distribution. The phenomenon of transition is comparable to that of nucleation of crystals, i.e., once a cell has collapsed, its surroundings cells begin to collapse, until all the cells of the sample have completed the transition phase. Having completed the transient phase, the applied stress value becomes constant and usually named as Maxwell Stress. Figure 3b consists of three digital images where the phenomenon can be observed. This model showed consistency with the deformation tests coaxial to the growth direction of the foams [30].

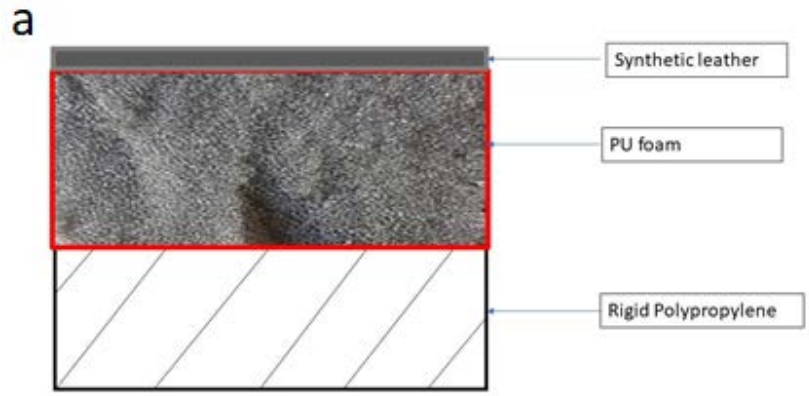

Figure 3. *Cont.*

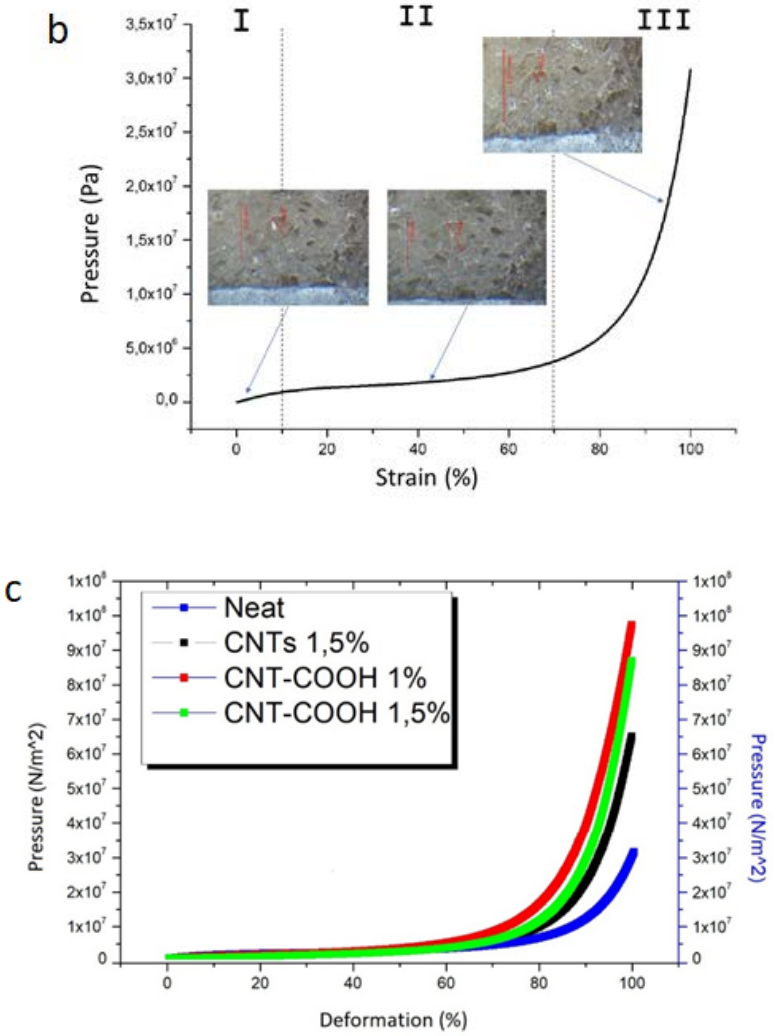

Figure 3. (**a**) Cross section of the designed sandwich structure (sample size: D 4.5 cm, thickness (thk) 1 cm). (**b**) The typical stress-strain curve of the prepared foam. (**c**) Mechanical compression test versus deformation for different types of foam (sample size: D 4.5 cm, thk 1 cm).

Figure 3c demonstrates the results of the compression test applied on the neat foam, as well as the foam with different percentages of CNT-COOH and CNT additives. The data for Elastic modulus and the engineering curves was obtained mediating results of 3 samples obtained by 3 different PU foams for each typology. The most rigid foam was obtained by adding 1.5 wt % of CNT-COOH at the polyol. Table 1 shows the elastic modulus of the sample calculated in the plateau region. One percent of CNT added to the neat foam increases the rigidity, while reducing the mechanical strength, compared to the CNT/COOH with a lower concentration. The foam prepared with CNT-COOH exhibited the highest elastic modulus compared to the foam obtained with neat PU and PU/CNT 1.5 wt %.

Table 1. Comparison among the elastic's modulus of different sample with CNT concentration.

PU sample	$E_{plateau}$ (MPa)
Neat PU	31
PU/CNT 1.5%	42
PU/CNT-COOH 1%	45
PU/CNT-COOH 1.5%	52

3.3. Piezoresistive Tests

Preliminary electromechanical compression test was performed on the PU foam sample while the electrical resistance and the deformation were acquired, simultaneously. Figure 4a displays the experimental results of the deformation versus time (resistance) of PU/CNT 1.5% subjected to the preliminary compression test. The samples showed conductivity even without applying the compression test, where the corresponding resistance was about 90MOhm. The electrical resistance gradually decreased with the imposed deformation from 0% to 99.8% of compression. Figure 4b depicts the experimental results of the compression test for PU/CNT-COOH 1%. Neat polyurethane disks have a resistance higher than 120 MOhm. Moreover, the PU foam samples with CNT-COOH of 1 % were considered insulating material when not loaded. However, the PU/CNT-COOH 1% disks showed a continuous insulator–conductor transition during the compression test, while the electric resistance dramatically dropped by 629 kOhm at 95.5% of deformation. After 10 min of being under the compression load at 95.5% of compressive strain, the samples began to show a stable and constant value of electric resistance equal to 618 kOhm. The electrical resistance steadily decreased under the imposed deformation from the 95.5% to the 99.8% of the compression strain.

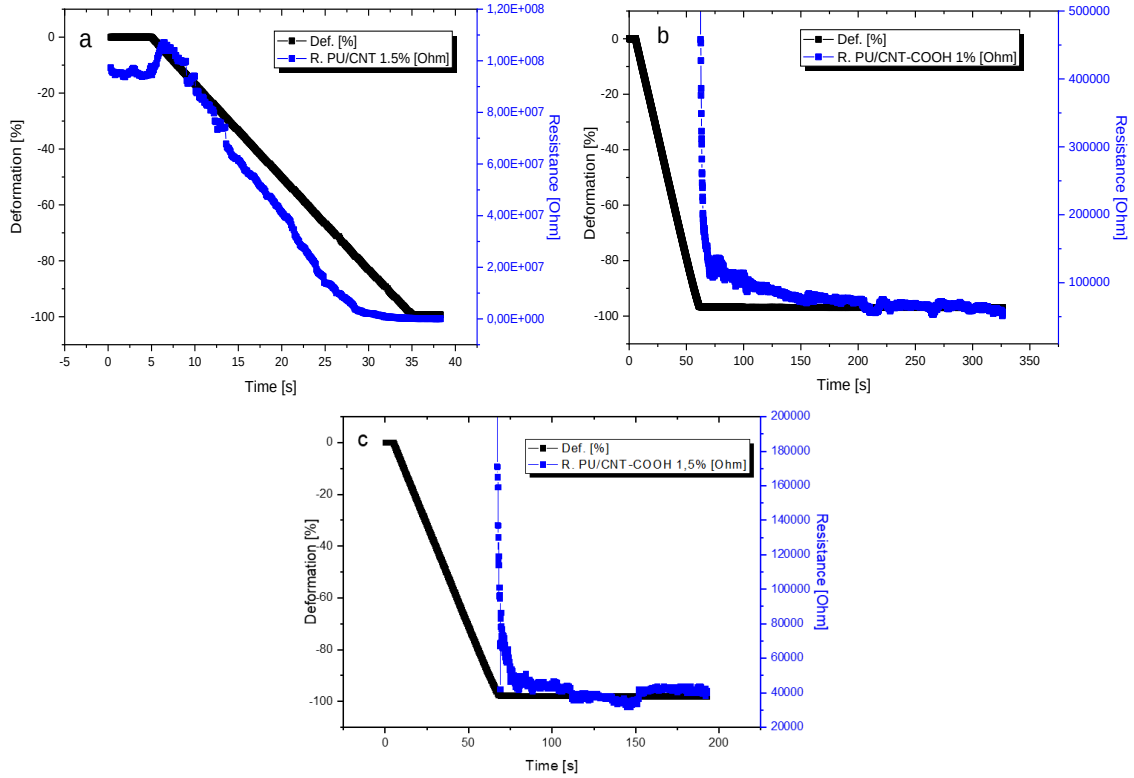

Figure 4. Experimental results of deformation-time and electrical resistance-time graph of (**a**) PU/CNT 1.5%, (**b**) PU/CNT-COOH 1%, and (**c**) PU/CNT-COOH 1.5% under compression test. (samples size: D 4.5 cm, thk 1 cm).

Figure 4c shows the result obtained during the preliminary compression test of PU/CNT-COOH 1.5%. As in the case of PU/CNT-COOH 1%, the disks made with PU/CNT-COOH 1.5% showed a continuous insulator–conductor transition during the compression test, while the electric resistance experienced a dramatic fall by 39 kOhm at 95.5% of deformation. The samples, after 10 min of being under compression loading, reached to a stable resistance value of 34kOhm at 95.5% of deformation. The electrical resistance gradually decreased with the imposed deformation from 95.5% to 99.8% under compression loading.

The linear behavior of the electric resistance with the imposed displacement of the sample made with CNT could be explained with an optimum dispersion of CNT (as showed in SEM analysis) in physical contact with each other. In this case, the total resistance of the sensor is mainly due to the contact resistance of CNT, as explained in Reference [31]. On the contrary, the trend of the electrical resistance of sample made with CNT-COOH is exponential and can be explained by Simmons's law [32]:

$$R_{tunnel} \sim d\, e^{d} \quad (1)$$

where d is the distance between CNT, and R_{tunnel} is the tunnelling resistance. The behavior of the sample with CNT-COOH is typical of sensors in which CNT are aggregated. In this case, the conductive path is dominated by tunnelling resistance among agglomerates. Table 2 gives information about the data related to the insulator-conductor transition.

Table 2. Deformation range, initial resistance value, and final resistance value of PU foams that exhibited insulator-conductor transition.

PU foam	Deformation Range (%)	Initial Resistance Value (MOhm)	Final Resistance Value (kOhm)
PU CNT-COOH 1%	95.5–99.8	>120 [1]	618
PU CNT-COOH 1.5%	95.5–99.8	>120 [1]	34

[1] The maximum instrument threshold.

3.4. Cyclic Compressive Loading

The samples were subjected to cyclic test to investigate their electromechanical behavior under cyclic deformations. The electric signal became steady and more stable when the sample were compressed over 90% of the initial thickness. Therefore, the cyclic compressive loading was applied on the compressed samples, in which value of compression depends on the kind of sample, to obtain stable electrical signals, avoiding resistance relaxation behavior, and comparing both filler CNT with CNT-COOH. The electrical resistance of composite foam at 99.8% of compression strain was chosen as the initial resistance (R_0) in order to evaluate the piezoresistive behavior starting from the condition of maximum compressibility. This test was aimed to test the foam as a sensor and/or switch application inside a hypothetic innovative smart dashboard. All tests were conducted by compressing the foam samples and waiting 10 min for stabilizing signals. Figure 5a illustrates 5 cycles of PU/CNT 1.5% and the variations of the corresponding electrical resistances under cyclic loadings. The black line indicates the compression strain which varies of 10%, and the blue line is the electrical resistance that changes with the imposed compression. The compression strain oscillated between 90% and 99.8%, in coordination with the electric resistance signal. The highest value reached by the resistance variation was 8900%. Figure 5b displays 5 cycles of PU/CNT-COOH 1% where the electrical resistance changes accordingly with the imposed compression. The black line indicates the compression strain, and the blue line is the electrical resistance variation that changes with the imposed compression. In this specific case, compression strain ranged from 95.5% to 99.8%, with an amplitude of 4.3%, in coordination with the electric resistance variation that oscillated between 750% and 100%.

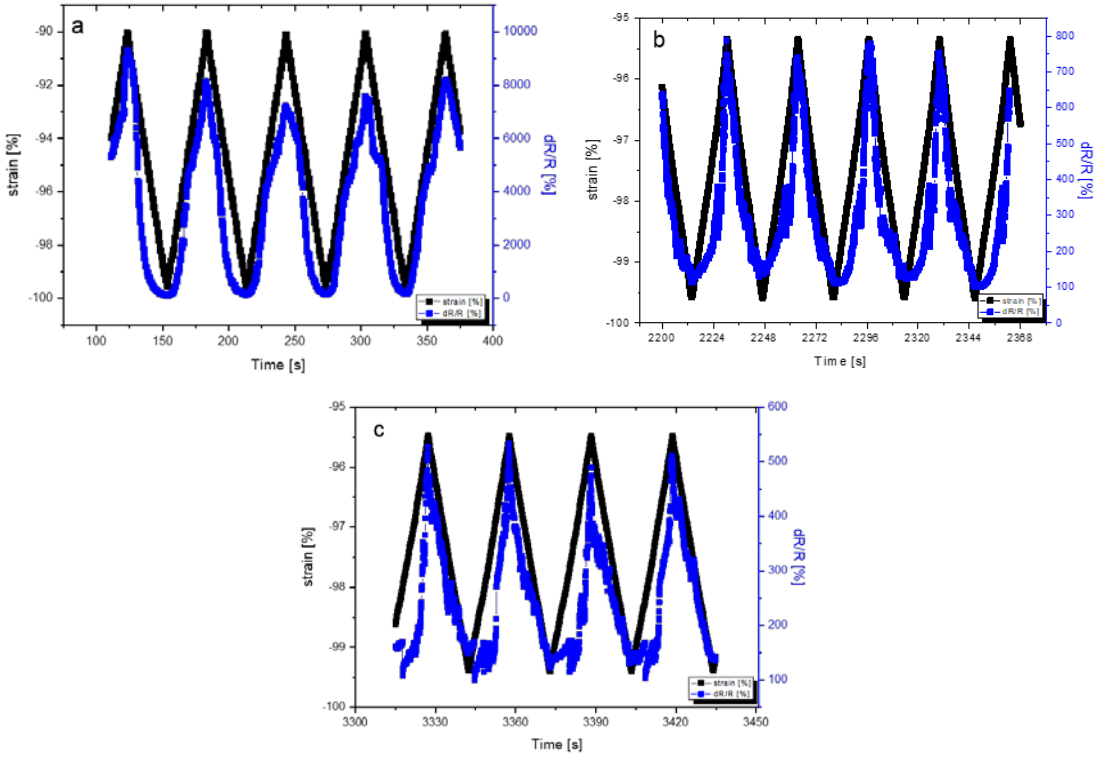

Figure 5. Cyclic electromechanical tests at average velocity of 2 mm/min of (**a**) PU/CNT 1.5% (sample size: D 4.5 cm, thk 1 cm), and (**b**) PU/CNT-COOH 1% (sample size: D 4.5 cm, thk 1 cm). (**c**) PU/CNT-COOH 1.5% (sample size: D 4.5 cm, thk 1 cm).

Figure 5c lines chart shows 4 cycles of PU/CNT-COOH 1.5%, where the electrical resistance changes accordingly with the imposed compression. The black line indicates the compression strain, and the blue line is the electrical resistance variation that changes with the imposed compression. In this specific case, compression strain ranged from 95.5% to 99.8%, with an amplitude of 4.3%, in coordination with the electric resistance variation that oscillates between 750% and 100%.

PU CNT and PU CNT-COOH foams were subjected to a fixed cyclic deformation (from 0% to 4%), while the multimer acquired the electrical resistance for many cycles, in order to test the durability and reliability of the piezoresistive response of different PU foams. Figure 6 shows a detail of this experimental test. The two different shape of the signal suggested, again, two different types of electrical conduction (contact and tunnelling) inside the two distinctive percolative network with CNT or CNT-COOH.

Different piezoresistive foams also exhibit different sensitivity. Table 3 shows the Gauge Factor of produced PU foams. The initial length of the sensors considered in the calculation was the thickness of the foam compressed at 99.8%. Moreover, the final elongation coincided with the insulator-conductor transition length.

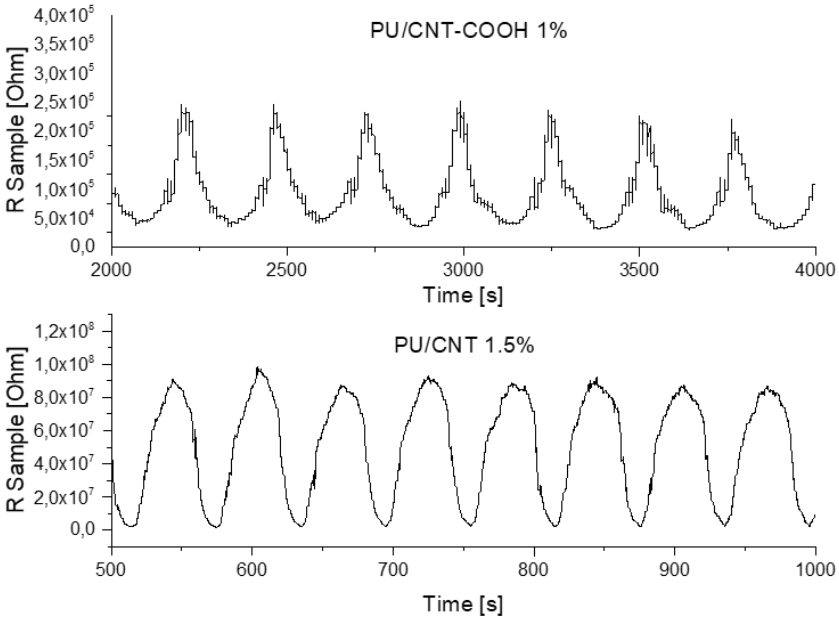

Figure 6. Details of durability piezoresistive tests on PU CNT-COOH 1% (first graph) and PU CNT 1.5% (second graph) (sample size: D 4.5 cm, thk 1 cm).

Table 3. The gauge factor result from tested samples.

PU foam	Gauge Factor
PU CNT 1.5%	80
PU CNT-COOH 1%	33
PU CNT-COOH 1.5%	23

4. Discussion

Different composite PU foams were characterized to evaluate their applicability as smart sensor or switch. All the produced samples showed a clear piezoresistive effect. The conductive fillers treated with this purpose were CNT and CNT-COOH. The fillers were dispersed inside a commercial polyol solution furnished as component of commercial BASF product. The applied base components were the same used in the industrial foaming process. The dispersion of CNT inside a polymer matrix is a complex problem that involves several parameters [33–35]. The most important are the dispersion method (sonication, calendaring, ball milling, shear mixing, extrusion) and the CNT dimension and functionalization. Regardless of which dispersion technique is used, the major obstacle is the surface interaction of the CNT with the polymer matrix. In fact, the interaction forces among CNT, such as electrostatic and Van Der Waals forces, are responsible for agglomeration phenomena. Furthermore, the CNT surface area enormously raises with decreasing of dimensions of CNT, causing a much stronger agglomeration problem [34,35]. Research has shown that CNT during dispersion are subjected to high shear forces and get damaged and broken [35]. The hypothesis is that CNT-COOH are more brittle than raw CNT because functionalization process induced defect on the CNT surface [36]. The sonication phase should increase CNT-COOH surface area much more than raw CNT improving the agglomeration phenomena [35]. Furthermore, the presence of CNT, with or without functionalization, slightly increases the mechanical rigidity of the foam respect to the neat PU. Generally, nanocomposites polymers reinforced with CNT have shown highest compressive elastic modulus and strength respect to the polymeric matrices [22–24]. These increase in mechanical properties is mainly due to the interface interaction between the matrix and CNT [37]. In this case, the external load applied to the PU/CNT foam is transferred from the polyurethane chains to the CNT

and, the more efficient the transfer, the more CNT will take part in the compression process and in the resulting increased mechanical properties. Moreover, the electrostatic interactions and the linking between the nanotubes impedes the evolution of the cracks [23]. PU foam samples showed also electrical conductivity and piezoresistivity. The percolation theory [6,38] can be applied to explain the electrically conducting behavior of composites consisting of conducting fillers and insulating matrices. When the conducting filler content gradually increased, the composite undergoes an insulator-to-conductor transition and the concentration of filler at the transition is called percolation threshold [39,40]. In addition, nanocomposites similar to PU/CNT foams showed an electrical resistance change when subjected to a strain [38,40,41]. In this condition, the conductive network inside the polymers changes its morphology because polymer chains cause fillers sliding [41], resulting in a resistance increase or decrease depending on the kind of strain. The resistance-strain correlation of the final nanocomposite PU foam strongly depends on the functionalization of CNT in terms of intensity and insulator-conductor transition phenomena. In particular, CNT showed lower electrical resistance value, and it was possible to make a conductive and piezoresistive PU foam without applying any deformation. On the contrary, the CNT-COOH conductive network formed inside the PU matrix showed high resistance value. In addition, the electric resistance can be revealed only if the specimens were subjected to a deformation higher than 90% of compression strain. Similarly, the resistance-strain responses of PU/CNT 1.5% and PU/CNT COOH 1% were completely different. The modification of CNT are supposed to improve solubility and processability [42], so it could provide a more finely distributed network inside the material that is needful to get the electron flow through the polymer [43]. On the other hand, surface modification of CNT could affect sp2 domains [36], increasing the number of defects on the surface and breaking π bond during the reaction, leading to a decreasing electron flow. The functionals groups could affect the electron flow in two opposite ways. We observed that the dispersion obtained with CNT-COOH was not better than the one obtained with CNT. However, the alteration of sp2 domain is not compensated by a denser network of filler inside the material and the final effect of using modified CNT is a lower electrical performance of the device. All the samples with non-functionalized CNT showed a linear response in correlation with the compressive strain and the highest Gf, which usually is a more desirable features for sensing applications. However, the composite foams did not show any conductor-insulator transition that could be a strategic feature in the case of switching application. The PU/CNT-COOH sample demonstrated a completely different behavior. In fact, samples showed conductor-insulator transition during compression. However, we found an extremely low Gf for PU-CNT-COOH compared to PU-CNT foams also the correlation between the resistance and strain was not completely linear. These features are commonly more suitable for less demanding application, as switches or on-off controllers, instead of sensing application.

5. Conclusions

We fabricated piezoresistive PU/CNT semi-rigid foam with the aim to investigate the possibility of obtaining a new production process for switches or sensors fully integrated with the material of a plastic component. Our method was developed for the automotive field but could be applied also in household appliance or home automation. For this purpose, nanomaterials foams were produced with a simple method compatible with a modern production system. Conductive CNT fillers were able to improve the electrical conductivity and mechanical property compared to the matrix alone. The experimental variables that were most taken into consideration were the functionalization of the CNT (which were supposed to influences their dispersion) and the composition of the polyurethane formulation. Contrary to our initial hypothesis, the composites obtained using CNT-COOH have shown a worse dispersion with respect to PU/CNT foam. SEM images revealed agglomerates in all CNT-COOH sample and a finer dispersion for PU/CNT foam. Moreover, PU/CNT-COOH foams showed, during the compression tests, an insulator-conductor transition that could be useful for switching application. In conclusion, promising results were achieved, even though the results have to be improved to achieve a finished product that should be produced at the industrial level. After all,

the possibility of developing expanded nanocomposites that have combine functional piezoresistive properties with structural ones inside a plastic component (i.e,. automotive dashboard) has been demonstrated. Moreover, we observed a new electrical effect, the insulator-conductor transition, never shown in PU/CNT composite foam. The next steps will be aimed at optimizing the preparation techniques in order to obtain homogeneous foams, both in dispersion and in properties. It will be necessary to evaluate new types of matrices, with a view to sustainability; for example, we could investigate thermoplastic polyurethanes and thermoplastic polymers in general. Finally, another interesting aspect emerged from this work was the not so high performance of the composites made; future research could be aimed to investigate the relation between device performances and quality of CNT.

Author Contributions: Conceptualization, E.D.M. and M.Z.; methodology, E.D.M.; software, E.D.M. and A.V.; validation, E.D.M., V.B., S.A.; formal analysis, E.D.M. and M.Z.; investigation, E.D.M.; resources, E.D.M.; data curation, E.D.M., S.A.; writing—original draft preparation, E.D.M., S.A. and M.Z.; writing—review and editing, E.D.M., V.B. and M.Z.; visualization, A.V.; supervision, E.D.M.; project administration, M.Z. and A.V.; All authors have read and agreed to the published version of the manuscript.

Funding: This research received no external funding.

Conflicts of Interest: The authors declare no conflict of interest.

References

1. Chatterjee, S.; Nafezarefi, F.; Tai, N.H.; Schlagenhauf, L.; Nüesch, F.A.; Chu, B.T.T. Size and synergy effects of nanofiller hybrids including graphene nanoplatelets and carbon nanotubes in mechanical properties of epoxy composites. *Carbon* **2012**, *50*, 5380–5386. [CrossRef]
2. Müller, M.T.; Krause, B.; Kretzschmar, B.; Pötschke, P. Influence of a supplemental filler in twin-screw extruded PP/CNT composites using masterbatch dilution. *AIP Conf. Proc.* **2019**, *2055*. [CrossRef]
3. Li, C.; Isshiki, N.; Saito, H.; Kohno, K.; Toyota, A. Nucleation effect of cyclodextrin inclusion complexes on the crystallization of isotactic poly (1-butene). *J. Polym. Sci. B Polym. Phys.* **2010**, *48*, 389–395. [CrossRef]
4. Yang, S.Y.; Lin, W.N.; Huang, Y.L.; Tien, H.W.; Wang, J.Y.; Ma, C.C.M.; Li, S.M.; Wang, Y.S. Synergetic effects of graphene platelets and carbon nanotubes on the mechanical and thermal properties of epoxy composites. *Carbon* **2011**, *49*, 793–803. [CrossRef]
5. Yu, J.; Choi, H.K.; Kim, H.S.; Kim, S.Y. Synergistic effect of hybrid graphene nanoplatelet and multi-walled carbon nanotube fillers on the thermal conductivity of polymer composites and theoretical modeling of the synergistic effect. *Compos. Part A Appl. Sci. Manuf.* **2016**, *88*, 79–85. [CrossRef]
6. Pötschke, P.; Bhattacharyya, A.R.; Janke, A. Carbon nanotube-filled polycarbonate composites produced by melt mixing and their use in blends with polyethylene. *Carbon* **2004**, *42*, 965–969. [CrossRef]
7. Wang, X.H.; Mu, Y.H.; Tang, Q.; Li, C.Q. Preparation and Performance of PVC/CNT Nanocomposite. *Adv. Polym. Technol.* **2018**, *37*, 358–364. [CrossRef]
8. Pereira, E.C.L.; Soares, B.G.; Silva, A.A.; da Silva, J.M.F.; Barra, G.M.O.; Livi, S. Conductive heterogeneous blend composites of PP/PA12 filled with ionic liquids treated-CNT. *Polym. Test.* **2019**, *74*, 187–195. [CrossRef]
9. Zare, Y.; Rhee, K.Y. The effective conductivity of polymer carbon nanotubes (CNT) nanocomposites. *J. Phys. Chem. Solids* **2019**, *131*, 15–21. [CrossRef]
10. Sang, Z.; Ke, K.; Manas-Zloczower, I. Effect of carbon nanotube morphology on properties in thermoplastic elastomer composites for strain sensors. *Compos. Part A Appl. Sci. Manuf.* **2019**, *121*, 207–212. [CrossRef]
11. Cesano, F.; Rattalino, I.; Demarchi, D.; Bardelli, F.; Sanginario, A.; Gianturco, A.; Veca, A.; Viazzi, C.; Castelli, P.; Scarano, D.; et al. Structure and properties of metal-free conductive tracks on polyethylene/multiwalled carbon nanotube composites as obtained by laser stimulated percolation. *Carbon* **2013**, *61*, 63–71. [CrossRef]
12. Ke, K.; Bonab, V.S.; Yuan, D.; Manas-Zloczower, I. Piezoresistive thermoplastic polyurethane nanocomposites with carbon nanostructures. *Carbon* **2018**, *139*, 52–58. [CrossRef]
13. Cravanzola, S.; Haznedar, G.; Scarano, D.; Zecchina, A.; Cesano, F. Carbon-based piezoresistive polymer composites: Structure and electrical properties. *Carbon* **2013**, *62*, 270–277. [CrossRef]
14. Li, J.; Orrego, S.; Pan, J.; He, P.; Kang, S.H. Ultrasensitive, flexible, and low-cost nanoporous piezoresistive composites for tactile pressure sensing. *Nanoscale* **2019**, *11*, 2779–2786. [CrossRef]

15. Bennett, J.W.; Thio, T.; Hiura, H.; Lezec, H.J.; Ebbesen, T.W.; Ghaemi, H.F. Electrical conductivity of individual carbon nanotubes. *Nature* **2003**, *382*, 54–56. [CrossRef]
16. Theodosiou, T.C.; Saravanos, D.A. Numerical investigation of mechanisms affecting the piezoresistive properties of CNT-doped polymers using multi-scale models. *Compos. Sci. Technol.* **2010**, *70*, 1312–1320. [CrossRef]
17. Hu, N.; Karube, Y.; Yan, C.; Masuda, Z.; Fukunaga, H. Tunneling effect in a polymer/carbon nanotube nanocomposite strain sensor. *Acta Mater.* **2008**, *56*, 2929–2936. [CrossRef]
18. Caradonna, A.; Badini, C.; Padovano, E.; Veca, A.; De Meo, E.; Pietroluongo, M. Laser Treatments for Improving Electrical Conductivity and Piezoresistive Behavior of Polymer–Carbon Nanofiller Composites. *Micromachines* **2019**, *10*, 63. [CrossRef]
19. Liu, H.; Gao, J.; Huang, W.; Dai, K.; Zheng, G.; Liu, C.; Shen, C.; Yan, X.; Guo, J.; Guo, Z. Electrically conductive strain sensing polyurethane nanocomposites with synergistic carbon nanotubes and graphene bifillers. *Nanoscale* **2016**, *8*, 12977–12989. [CrossRef]
20. Abishera, R.; Velmurugan, R.; Gopal, K.V.N. Reversible plasticity shape memory effect in carbon nanotube/epoxy nanocomposites: Shape recovery studies for torsional and bending deformations. *Polym. Eng. Sci.* **2018**, *58*, E189–E198. [CrossRef]
21. Elwi, T.A.; Al-Rizzo, H.M.; Rucker, D.G.; Dervishi, E.; Li, Z.; Biris, A.S. Multi-walled carbon nanotube-based RF antennas. *Nanotechnology* **2010**, *21*. [CrossRef]
22. Xu, X.-B.; Li, Z.-M.; Shi, L.; Bian, X.-C.; Xiang, Z.-D. Ultralight Conductive Carbon-Nanotube–Polymer Composite. *Small* **2007**, *3*, 408–411. [CrossRef] [PubMed]
23. Yan, D.-X.; Dai, K.; Xiang, Z.-D.; Li, Z.-M.; Ji, X.; Zhang, W.-Q. Electrical conductivity and major mechanical and thermal properties of carbon nanotube-filled polyurethane foams. *J. Appl. Polym. Sci.* **2011**, *120*, 3014–3019. [CrossRef]
24. Tewari, A.; Gandla, S.; Bohm, S.; McNeill, C.R.; Gupta, D. Highly Exfoliated MWNT-rGO Ink-Wrapped Polyurethane Foam for Piezoresistive Pressure Sensor Applications. *ACS Appl. Mater. Interfaces* **2018**, *10*, 5185–5195. [CrossRef] [PubMed]
25. Zhai, T.; Li, D.; Fei, G.; Xia, H. Piezoresistive and compression resistance relaxation behavior of water blown carbon nanotube/polyurethane composite foam. *Compos. Part A Appl. Sci. Manuf.* **2015**, *72*, 108–114. [CrossRef]
26. Leifer, N.D.R.; Noked, M.; Nessim, G.D. A straightforward and reliable method for the characterization of carbon nanotube dispersions. *Carbon* **2010**, *49*, 1042–1047. [CrossRef]
27. Icoglu, F.; Ciltas, A.; Simsek, N. Chemosphere A holistic study on potential toxic effects of carboxylated multi-walled carbon nanotubes (MWCNTs-COOH) on zebra fi sh (Danio rerio) embryos/larvae. *Chemosphere* **2019**, *225*, 820–828. [CrossRef]
28. Bai, J.; Goodridge, R.D.; Hague, R.J.M. Nanostructural characterization of carbon nanotubes in laser-sintered polyamide 12 by 3D-TEM. *J. Mater. Res.* **2014**, 1817–1823. [CrossRef]
29. Michel, T.R.; Capasso, M.J.; Cavusoglu, M.E.; Decker, J.; Zeppilli, D.; Zhu, C.; Bakrania, S.; Kadlowec, J.A.; Xue, W. Evaluation of porous polydimethylsiloxane/carbon nanotubes (PDMS/CNTs) nanocomposites as piezoresistive sensor materials. *Microsyst. Technol.* **2020**, *26*, 1101–1112. [CrossRef]
30. Gioia, G. Experiments on Elastic Polyether Polyurethane Foams Under Multiaxial Loading: Mechanical Response and Strain Fields. *J. Appl. Mech.* **2011**, *78*, 031018. [CrossRef]
31. Hu, N.; Fukunaga, H.; Atobe, S.; Liu, Y.; Li, J. Piezoresistive Strain Sensors Made from Carbon Nanotubes. *Sensors* **2011**, *11*, 10691–10723. [CrossRef]
32. Simmons, J.G. Generalized Formula for the Electric Tunnel Effect between Similar Electrodes Separated by a Thin Insulating Film. *J. Appl. Phys.* **1963**, *34*, 6. [CrossRef]
33. Ma, P.; Siddiqui, N.A.; Marom, G.; Kim, J. Composites: Part A Dispersion and functionalization of carbon nanotubes for polymer-based nanocomposites: A review. *Compos. Part A Appl. Sci. Manuf.* **2010**, *41*, 1345–1367. [CrossRef]
34. Sahoo, N.G.; Jung, Y.C.; Yoo, H.J.; Cho, J.W. Effect of Functionalized Carbon Nanotubes on Molecular Interaction and Properties of Polyurethane Composites. *Macromol. Chem. Phys.* **2006**, *207*, 1773–1780. [CrossRef]

35. Foundation, A.; Blaedel, W.J.; Wang, J.; Rochon, A.M.; Gesser, H.D.; Aubert, J.H.; Rand, P.B.; Arnold, C.; Clough, L.R.; Clough, R.L.; et al. Mechanical Damage of Carbon Nanotubes by Ultrasound. *Carbon* **1996**, *34*, 814–816.
36. Liu, P. Modifications of carbon nanotubes with polymers. *Eur. Polym. J.* **2005**, *41*, 2693–2703. [CrossRef]
37. Spitalsky, Z.; Tasis, D.; Papagelis, K.; Galiotis, C. Progress in Polymer Science Carbon nanotube—Polymer composites: Chemistry, processing, mechanical and electrical properties. *Prog. Polym. Sci.* **2010**, *35*, 357–401. [CrossRef]
38. Mutlay, İ.; Tudoran, L.B. Percolation Behavior of Electrically Conductive Graphene Nanoplatelets/Polymer Nanocomposites: Theory and Experiment. *Fuller. Nanotub. Carbon Nanostruct.* **2014**, *4046*. [CrossRef]
39. Zhang, R.; Dowden, A.; Deng, H.; Baxendale, M.; Peijs, T. Conductive network formation in the melt of carbon nanotube/thermoplastic polyurethane composite. *Compos. Sci. Technol.* **2009**, *69*, 1499–1504. [CrossRef]
40. Yan, T.; Wang, Z.; Pan, Z. Flexible strain sensors fabricated using carbon-based nanomaterials: A review. *Curr. Opin. Solid State Mater. Sci.* **2018**, *22*, 213–228. [CrossRef]
41. Avil, F.; Cen-Puc, M. Piezoresistivity, Strain, and Damage Self-Sensing of Polymer Composites Filled with Carbon Nanostructures. *Adv. Eng. Mater.* **2018**, *20*, 1701159. [CrossRef]
42. Fu, K.; Sun, Y. Dispersion and Solubilization of Carbon Nanotubes. *J. Nanosci. Nanotechnol.* **2003**, *3*, 351–364. [CrossRef] [PubMed]
43. Kirkpatrick, S.; Thomas, I.B.M.; Heights, Y.; York, N. The nature of percolation 'channels'. *Solid State Commun.* **1973**, *12*, 1279–1283. [CrossRef]